J Med Dent Sci 2002; 49: 67–75

Original Article

Sequence of ultrastructural changes of enamel crystals and *Streptococcus mutans* biofilm in early enamel caries *in vitro*

Lina Naomi Hashizume[1)], Kayoko Shinada[1)], Yoko Kawaguchi[1)] and Yasuo Yamashita[2)]

1) Oral Health Promotion (Chairman: Prof. Yoko Kawaguchi), Department of International Health Development, Graduate School, Tokyo Medical and Dental University
2) Maxillofacial Anatomy (Chairman: Prof. Yasuo Yamashita), Department of Maxillofacial Biology, Graduate School, Tokyo Medical and Dental University

Undecalcified mature enamel sections were used to observe the sequence of ultrastructural changes of enamel crystals and *Streptococcus mutans* biofilm in the early stages of caries. Human enamel blocks were incubated from 1 to 7 days with *S. mutans* suspension, and the pH of biofilm was measured. They were processed for light microscopic and transmission electron microscopy observations, and the number of bacteria located in the area adjacent to enamel surface counted. It was observed that the pH of the biofilm dropped to 4, after 1-day of incubation and the *S. mutans* number increased until 4-day. Round shaped enamel crystals were observed in the 2-day specimens and from the 4-day, images of crystals showing defects and perforations were visualized, becoming more defective along the incubation days. The length of time that the enamel was exposed to biofilm was the main factor for enamel crystals demineralization. Current *in vitro* caries induction system could standardize time-related changes of the property of *Streptococcus mutans* biofilm and its relation to enamel crystals demineralization at the ultrastructural level, and thus provide a useful model for the evaluation of the effects of various anti-cariogenic agents.

Key words: Mature enamel crystals, *Streptococcus mutans* biofilm, ultrastructure, *in vitro* model system, bacteria counting.

Corresponding Author: Lina Naomi Hashizume
Oral Health Promotion, Department of International Health Development, Graduate School, Tokyo Medical and Dental University
1-5-45 Yushima, Bunkyo-ku, Tokyo, Japan 113-8549
Telephone number: 81-3-5803-5476
Fax number: 81-3-5803-0194
E-mail address: lhashizume@yahoo.com
Received February 7; Accepted March 22, 2002

Introduction

In dental caries, the demineralization of dental enamel is caused by acids produced from the fermentation of dietary carbohydrates by dental-plaque bacteria[1,2]. Mutans streptococci are considered as important cariogenic plaque organisms[3,4], particularly, *Streptococcus mutans* (*S. mutans*) which is implicated as a potent caries-conducive microorganism in man[5,6,7]. Plaque biofilm is a complex and dynamic environment and its relation with dental enamel is more than its adhesion on surfaces. Since caries development is a time-related process, the interaction between plaque biofilm and enamel crystals in the first stages of the carious process is important for understanding more about the mechanism of early enamel caries.

Mature human dental enamel has a high degree of mineralization making structural studies somewhat less straightforward than for other tissues, particularly for modes of imaging involving transmission electron microscopy. In the literature, only a few studies have reported the ultrastructure of sound dental enamel and

enamel affected by caries[8,9,10]. To section bacterial biofilm adhered to undecalcified mature enamel, a very careful technique is required because the difference of hardness between high mineralized enamel and soft biofilm makes ultra-cutting difficult. Accordingly, ultrastructural observations of bacterial biofilms adhered to undecalcified and mature enamel, and the sequence of events that occur in the early stages of caries, were not found in the literature, thus justifying this study.

The purpose of this study was to evaluate the chronological changes of *S. mutans* biofilm and human enamel crystals in the process of dental caries using a new *in vitro* model system. This new in vitro model system combined the use of *S. mutans* biofilm colonized on human enamel block surface and light and electron microscopic observations of its undecalcified sections. To verify the interaction between *S. mutans* biofilm and enamel crystals, the pH of the biofilm and the number of bacteria located in the area adjacent to enamel surface were also assessed.

Materials and methods

1. Samples preparation

Impacted human third molars were used in this study. Their crowns and the roots were cut using a low-speed diamond cutting saw (Isomet, Buehler Ltd., Lake Bluff, IL, USA) and the tooth surfaces were slightly polished by grinding with abrasive paper under running water down to grit size 3,000. Enamel blocks, measuring $3 \times 3 \times 2$ mm, were cut perpendicularly to the tooth surface using diamond disks under water. The blocks were cleaned ultrasonically and sterilized in an autoclave for 20 min at 120°C. Fifty-nine enamel blocks were prepared and used in this experiment. Paraffin-stimulated whole saliva samples were collected from the same healthy, non-smoking adult donor. Saliva was clarified by centrifugation 25,000 *g* for 15 minutes at 4°C[11,12] and filtered (Sterile Millex-HA, 0.20 μm filter unit, Millipore, MA). The enamel blocks were covered with this saliva and incubated at 37°C for 2 hours[13] and washed twice with phosphate buffer. Seven pellicle-coated blocks were reserved for controls in the TEM observations. Fifty-two pellicle-coated enamel blocks were attached to stainless steel wire using dental wax and each block was immersed into 10 ml of sterile brain-heart infusion broth (Difco Labs., Detroit, MI, USA) containing 5% sucrose to which 0.1 ml of an overnight starter culture of *Streptococcus mutans* NCTC 10449 (serotype c, from our laboratory strain) had been inoculated. Samples were incubated at 37°C for periods of 1, 2, 3, 4, 5, 6 and 7 days. The enamel blocks were transferred to fresh culture media every 24 hours to renew the environment, so providing nutrients to permit growth of the biofilms. Seven samples were prepared each day for microscopic observations (light microscope and TEM), and three for measurement of biofilm pH.

2. Measurement of biofilm pH

The pH of the biofilm which formed on the enamel surface was measured with a Beetrode® pH microelectrode model NMPH 2B (WPI Inc., Sarasota, FL, USA) and a SDR 2 reference electrode, in combination with an ORION 720A pH/ISE meter (Orion Research Inc., Boston, Mass. USA). The extremity of the microelectrode was placed on the block surface to measure the pH of the deep layer of biofilm. pH was measured at 1st, 2nd, 3rd, 4th, 5th, 6th and 7th day of incubation. Three sites were measured for each sample at each day. The microelectrode was calibrated in standard buffers at pH 7 and 4 before each measurement. The initial pH of the media was adjusted to 7.

3. Light microscopic observations and bacteria counting

After each incubation period, samples for microscopic observations were pre-fixed with 2.5% glutaraldehyde solution (0.1M sodium cacodylate buffer, pH 7.3) for 3 hours. They were rinsed twice with the same buffer and post-fixed in 2% osmic acid for 4 hours, dehydrated by serial transfer in ascending concentration of ethanol and embedded in Epon 812 (TAAB Lab., Reading, England). Undecalcified semi-thin sections ($300 \times 300 \times 1$ μm) were cut from seven different samples per incubation day. The sections were stained with 0.1% toluidine blue and observed under VANOX-S light microscope (Olympus Ltd., Tokyo, Japan). The cutting plane of the sections were perpendicular to the enamel block surface. Light micrographs were taken of each semi-thin section and the number of bacteria in the 10×300 μm area along the enamel block surface was counted. To facilitate the counting, this area was divided in 30 continuous squares of 100 μm^2 along the enamel block surface and the number of bacteria in each square counted. For the statistical analysis, the software program Statistical Package of Social Science (SPSS 10.0J) was used. One-way ANOVA and Tamhane test were run for statistical evaluation. The p value < 0.05 was

considered to indicate statistical significance.

4. Transmission electron microscopic observations

From each sample, undecalcified ultra-thin sections were cut perpendicularly to the enamel block surface with an Ultracut E ultramicrotome (Reichert-Jung Optische Werk AG, Wien, Austria) using diamond knives and observed using a transmission electron microscope (HITACHI H-800L) operating at 100 to 200 kV accelerating voltage. Part of the sections was stained manually with Watson and Reynolds method (uranyl acetate and lead citrate solution), for observation of bacteria morphology, and the other part left unstained, for observation of enamel crystals.

Results

1. pH of biofilm

Before the experiment the pH of the medium was set to 7 for all samples. In the 1st day of incubation the biofilm pH dropped to 4.18 ± 0.04 (mean of the three points pH measurements ± SD) and in the 2nd, 3rd, 4th, 5th, and 6th day of incubation, pH values of 4.30 ± 0.02, 4.38 ± 0.02, 4.35 ± 0.04, 4.57 ± 0.13 and 4.41 ± 0.01 were observed, respectively. The final value of biofilm pH observed in the 7th day of incubation was 4.60 ± 0.12.

2. Light microscopic observations and bacteria counting

In the 1-day specimens, a few isolated colonies with a loose distribution were dispersed on enamel block surface (Fig. 1a). Figure 2 shows the number of bacteria per 100 μm^2 located in the area adjacent to enamel surface over the incubation days. The 1-day biofilm showed the lowest bacteria number, 30.90 ± 24.24 (mean of bacteria number ± SD / 100 μm^2), when compared with specimens from 2-day to 7-day, and was statistically significant ($p < 0.001$). The 2-day and 3-day specimens showed similar images of formation and fixation of colonies on the enamel block surface with fusions among the colonies (Fig. 1b). The number of bacterial cells adjacent to enamel surface increased in the 2-day specimens to 45.89 ± 18.58 and in the 3-day specimens to 43.16 ± 20.42. The difference between the number for the 2-day and 3-day specimens was not significant, however, compared with 1, 4, 5, 6 and 7-day specimens, both specimens (2-day and 3-day) had significant differences ($p < 0.001$). In the 4-day specimens, parts of the enamel surface were covered by coalesced colonies, while others were covered irregularly (Fig. 1c). The 4-day specimens showed the highest number of bacteria, 61.23 ± 20.70, which was statistically significant when compared to 1, 2 and 3-day specimens ($p < 0.001$). In the 5-day specimens (56.06 ±13.28), *S. mutans* colonies covered the enamel surface more uniformly than the 4-day specimens and in the 6-day (57.87 ± 9.47) and 7-day (56.88 ± 7.16) specimens, the distribution became more regular than the other days (Fig. 1d). The number of bacteria among the 4, 5, 6 and 7-day specimens did not show significant differences.

3. TEM observations

In the control specimens, enamel crystals showed appearance of roughly flattened hexagons. A close contact and tightly packed arrangement of the crystals were observed. The enamel crystals of the prism head showed orientation running in the prism longitudinal axis. Within the prism head, the crystals were parallel each other. Crystals from the prism tail showed an orientation perpendicular to the prism longitudinal axis and parallel to the enamel block surface (Fig. 3a). Narrow prism sheaths were also observed in the control specimens. In the 1-day specimens, *S. mutans* cells showed clear cell walls and well-stained intracellular structures. Cytoplasm was granular and well-stained. The shape of the cells was round and they presented in pairs and short chains. Many cells in division were also visualized (Fig. 1e). The arrangement and orientation of the enamel crystals showed an appearance similar to the control (Fig. 3b). In the 2-day specimens, more *S. mutans* cells were observed on the enamel block surface and the bacterial chains were longer compared with the 1-day specimens. Several cells were seen in bacterial division (Fig. 1f). Light electronic stained substance was clearly verified in the intercellular spaces. The surface of the enamel crystals showed a loss of sharp symmetry at the poles (Fig. 3c) and intercrystal spaces and prism sheaths wider than the control and 1-day specimens. In the 3-day specimens, images of *S. mutans* cells were similar to those observed in the 2-day specimens. The electronic staining of the intercellular substance observed in these specimens was denser than the 2-day specimens. Round shaped enamel crystals, similar to the 2-day specimens, were observed. The space among the crystals and the prism sheaths became wider than the 2-day and their arrangement was not as tight as the control (Fig. 3d). In the 4-day specimens, more intercellular substance was found in the biofilm and the sub-

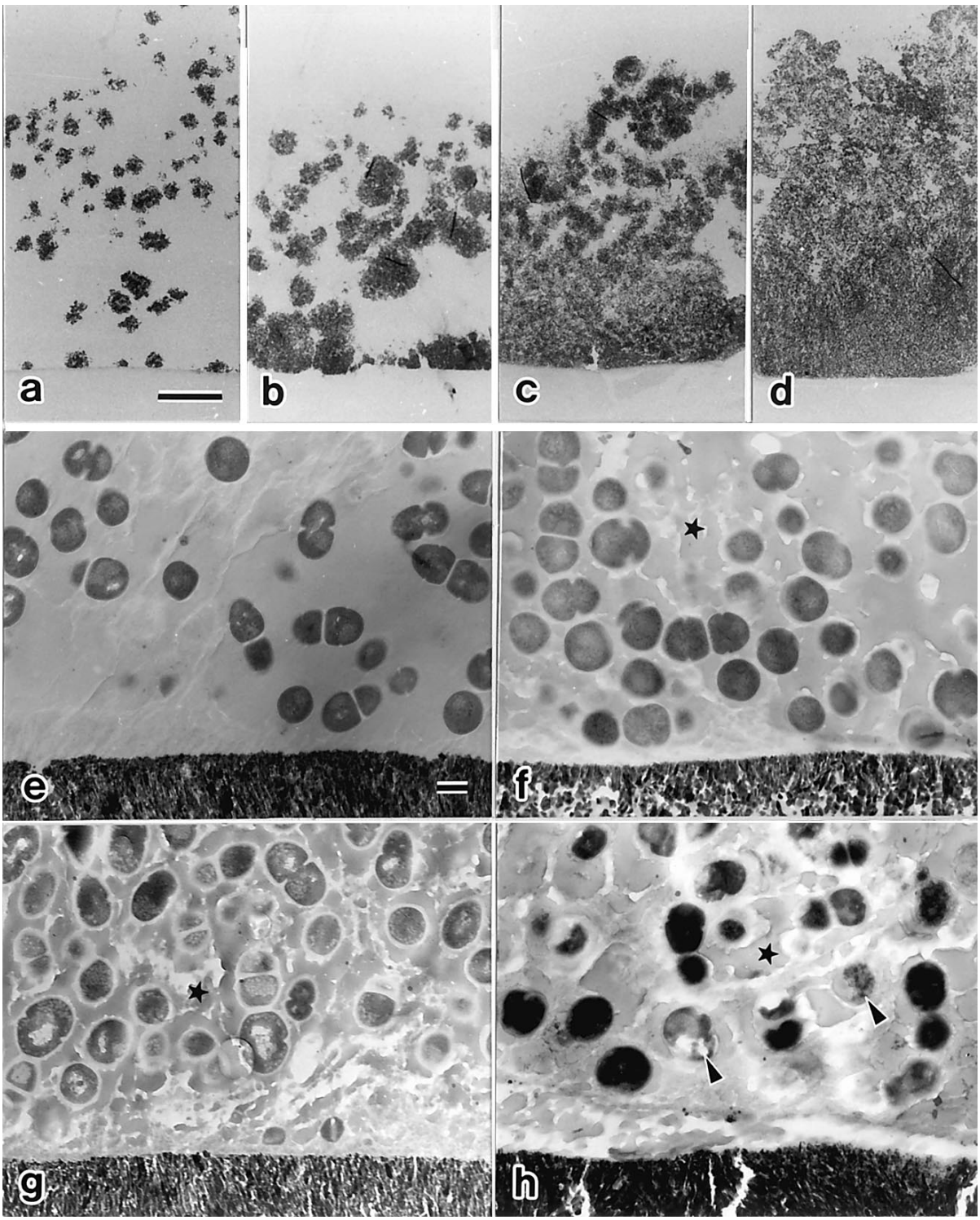

Fig. 1. Light micrographs of *S. mutans* biofilm distribution on enamel surface (a-d). In the 1-day specimens (a), isolated colonies with loose distribution are observed. Fixation and fusion among the colonies are seen in the 2-day specimens (b). 4-day (c) and 7-day (d) specimens show more uniform distribution of biofilm. Bar = 200 μm. Time-related changes in the ultrastructure of the *S. mutans* biofilm (e-h). The *S. mutans* cells of the 1-day specimens (e) have normal morphology with round shape, presenting in pairs or short chains. Light electronic stained substance (★) is clearly observed in the intercellular space of the 2-day specimens (f), becoming denser along the days. From the 4-day specimens (g), images of bacterial cells with abnormal shapes and light stained cytoplasm are observed. In the 7-day specimens (h), these cells are seen more often (arrowheads). Bar = 1 μm.

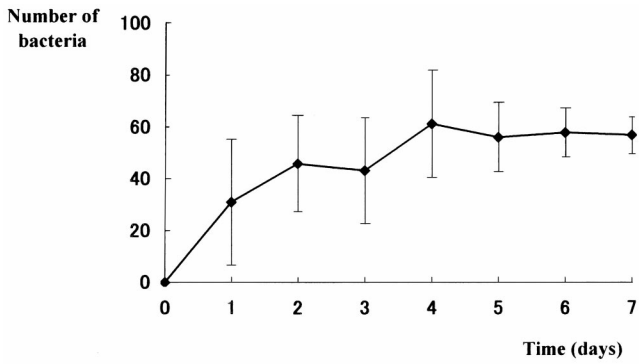

Fig. 2. Number (per 100 μm^2) of *Streptococcus mutans* cells located in the area adjacent to enamel surface over the incubation days.

stance located immediately above the enamel block surface, showed a granular appearance. Immersed into this substance, normal bacterial cells and some with abnormal shapes were seen (Fig. 1g). The enamel crystals were thinner than those of the 3-day specimens and some crystals showing central perforations and lateral defects were also visualized. The intercrystal spaces and prism sheaths were wider than the 3-day specimens. Orientation and arrangement of the crystals were irregular. Crystals located in the margin of prism sheaths (periphery of prism head) had an appearance larger and more symmetrical compared to the crystals of the prism head core (Fig. 4a). In the 5, 6 and 7-day specimens, bacteria with abnormal shapes became more numerous than normal shaped cells, in

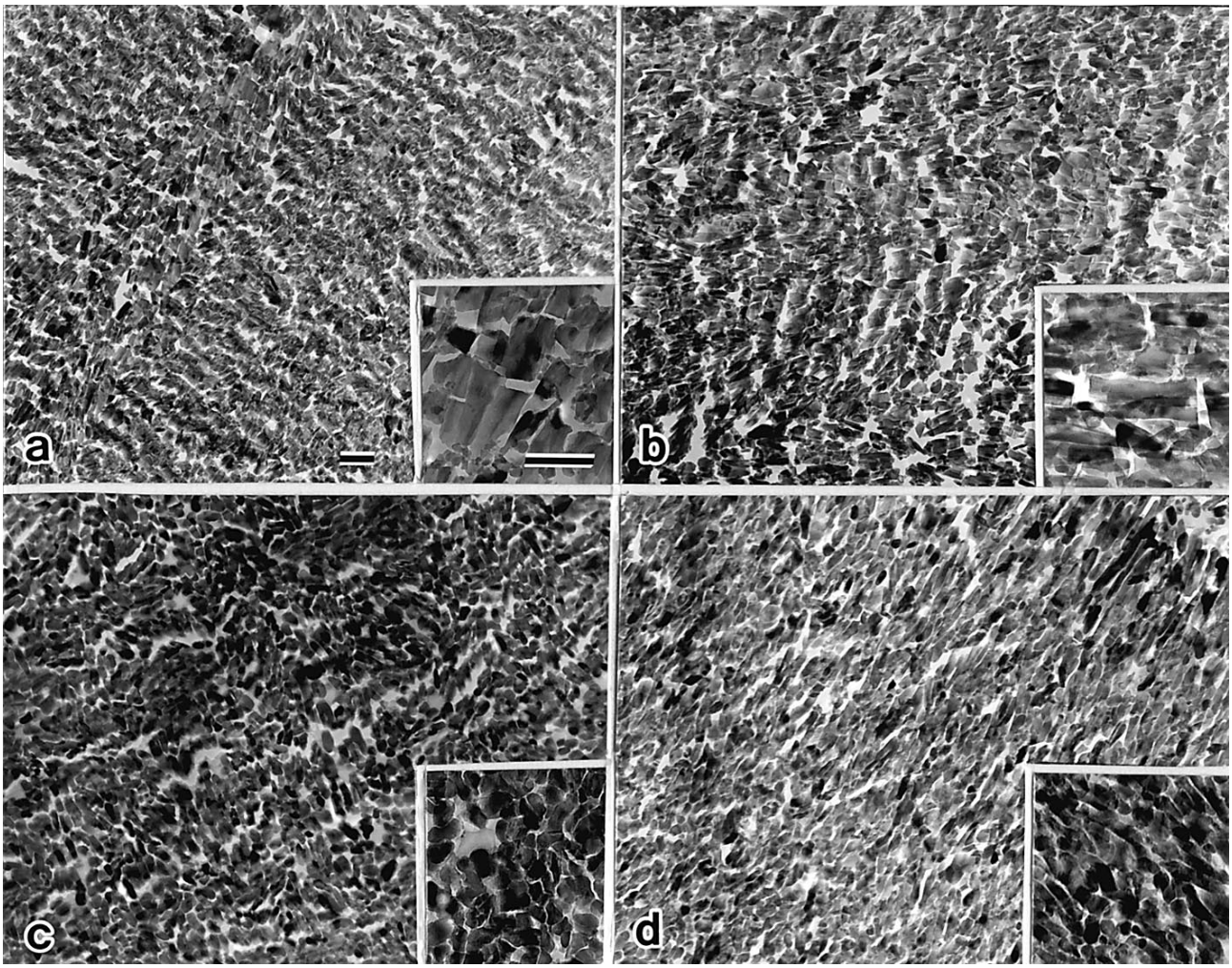

Fig. 3. TEM micrographs of the enamel crystals (a-d). The crystals of the control (a) and 1-day (b) specimens show similar features with sharp and roughly hexagonal appearance. In the 2-day (c) and 3-day (d) specimens are seen round shaped crystals and enlargement of intercrystal spaces. Bar = 1 μm. Enlarged view of crystals, from each day, is shown inset the pictures. Bar = 0.5 μm.

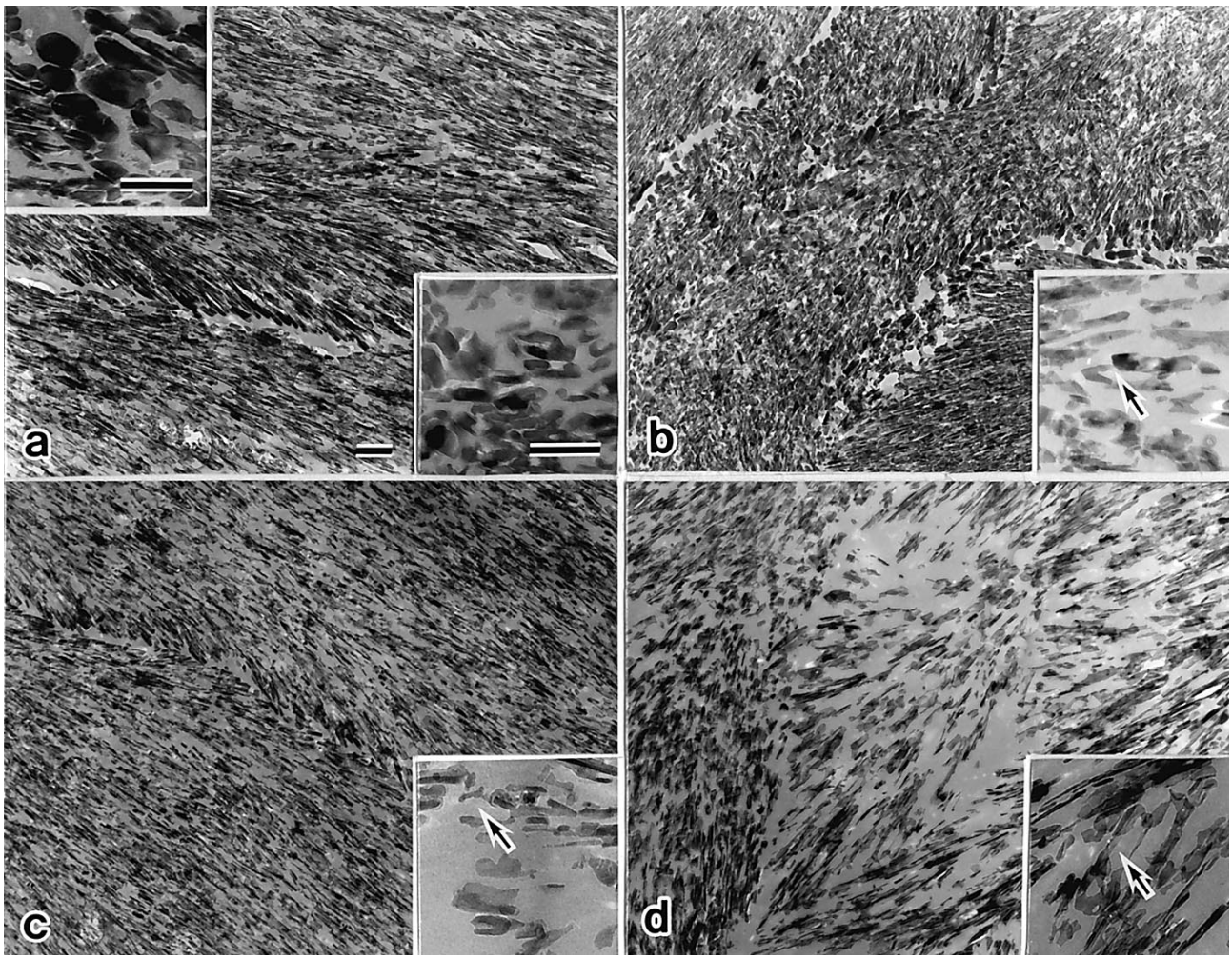

Fig. 4. Gradual changes of enamel crystals from 4-day to 7-day specimens (a-d). Thin and defective enamel crystals are seen in the 4-day specimens (a), becoming more numerous in the 5 (b), 6 (c) and 7-day (d) specimens. Bar = 1 μm. Enlarged view of enamel crystals is visualized inset each picture. Arrows indicate crystals with lateral defects and perforations. Bar = 0.5 μm. From 4-day specimens (a), crystals of the periphery of the prism head (upper inset) appear be larger than crystals from the central part.

the deep layers of biofilm. An increase of intercellular substance was verified over the days with bacterial cells embedded in, and located on, this substance. In the deep layers of the 7-day specimens, the biofilm showed many *S. mutans* cells with unclear cell walls, modified shapes and light electronic staining (Fig. 1h). The enamel crystals were becoming thinner, and more crystals showing central perforations and lateral defects were seen. Intercrystal spaces and prism sheaths became wider and the orientation of the crystals was more irregular in the biofilms of 6-day and 7-day specimens (Fig. 4 c,d).

Discussion

1. Changes of enamel crystals under *S. mutans* biofilm

The morphology of cross-sectioned crystals from sound mature enamel has been described as elongated and roughly flattened hexagons with sharp hexagonal symmetry at the poles[14,15]. The crystals seem to assume a size and shape necessary to fill all the available space and have narrow intercrystal spaces and prism sheaths[16,17,18]. Because of this, they possess a tightly packed arrangement, which has been described as a stoned wall arrangement[19]. When dental enamel is acid-treated or affected by natural or arti-

ficial caries, the crystals exhibit irregular shapes with superficial defects in various sizes and perforations in their centers[20,21,22]. Demineralization occurs first in the prism sheaths, and then in the core and in the periphery of prism head. These structures are considered susceptible to acidic attack[17]. The enlargement of prism sheaths and crystals located in the periphery of the prism head region with appearance somewhat larger and more equilaterally hexagonal than the crystals within the head of prisms also were observed in carious dental enamel[19,20,23].

In this study, the crystals of the enamel surface layer showed different features for shape, size and arrangement, according to the incubation period. Regarding shape and morphology, the enamel crystals exhibited a round shape in the 2-day and 3-day specimens, and in the 4-day specimens, they were thinner and showed lateral defects and perforations. These defective crystals became gradually more numerous until the 7-day specimens. Observation of these crystals indicated that demineralization had occurred, and confirmed the findings of other studies[9,22] that described crystals with similar features in carious enamel. The beginning of enlargement of intercrystal spaces and prism sheaths was observed in the 2-day specimens, and from the 4-day specimens, they were gradually becoming wider, and many crystals of the periphery of prism head appeared to be larger and more symmetric than the crystals in the central part of the head. The arrangement of the crystals became gradually loose from 4-day specimens. Our TEM observations have shown typical morphological features of carious enamel crystals, in the 4-day specimens. And, images of the beginning of crystal demineralization, such as crystals showing rounded shapes, could be seen in the 2-day specimens. The TEM results of the present study thus showed the main chronological features of enamel crystals, although the crystals of some areas remained similar to those of sound enamel. One explanation for this may be the existence of variables in the dental enamel, such as, level of prism mineralization, different prism orientation[17], and different patterns of bacterial colonization on the enamel surface[24].

2. Distribution of *S. mutans* and the pH profiles of biofilm

S. mutans uses fermentable sugars such as sucrose as a substrate for producing energy for their growth and reproduction, and has acids as final products of metabolism[6]. Our study showed that the number of *S. mutans* located in the area adjacent to enamel surface was increasing until the 4-day specimens, however its distribution on the surface was not regular. From the 4-day specimens, the number maintained stable and the distribution was becoming more uniform. The pH of the deep layers of biofilm dropped in the 1st day of incubation to values near pH 4, and in the following days it remained below 5, the critical pH below which teeth are increasingly at risk to carious attack[25]. Our findings are in accordance with those of Geddes[26] that reported that after exposure to sucrose, high concentrations of lactic acid rapidly build up in dental plaque, and pH decreases. It is known that *S. mutans* possess high acid tolerance[27] and as its typical pH minimums is about 3.9 to 4.05[28]. Thus, despite the fact that the pH of the biofilm was low, *S. mutans* could grow and reproduce, increasing its number and after becoming well distributed on enamel surface. Our TEM observations revealed some images of *S. mutans* cells with an unclear appearance from the 4-day specimens and clear lighter stained intercellular substance from the 2-day specimens in the area adjacent to enamel surface. These images became gradually more numerous over the days. These are in accordance to some studies[29,30] that related the existence of dead layers in the dental biofilm adjacent to the enamel surface, as being an integral component in the initial steps of biofilm formation. In this study, it was verified that a gradual increase of biofilm thickness occurred over the days. The increase of thickness may have made it difficult for the diffusion of nutrients from medium to deep layers of *S. mutans* biofilm, to take place, and is one reason for the appearance of dead layers. The increasing of the intercellular light stained substance and the uniform distribution of *S. mutans* from 4-day specimens, leads us to suppose that these substance may be the extracellular polysaccharides produced by *S. mutans* from sucrose, suggesting some relation with the production of this substance and its ability to adhere to the enamel surfaces.

3. Relationship between *S. mutans* biofilm and enamel crystals demineralization

It was possible to verify the interaction with *S. mutans* biofilm and demineralization of enamel crystals in our study. The initial changes of enamel crystal morphology were observed in the 2-day specimens, showing rounded shape crystals, however the typical morphological features for carious crystals were found in the 4-day specimens. The production of organic acids by bacteria and the subsequent lowering

of the pH at the enamel surface-plaque interface are required to initiate dental caries, however these may not be the decisive factors in caries causation[31]. Although the drop in pH occurred in the first day of incubation, images of the beginning of crystal demineralization were only observed in the 2-day specimens. An increase of bacterial cells leads to an increase of acid production and a uniform distribution on surface, results in the area attacked by acids becoming larger. Dibdin et al.[32] reported that extracellular polysaccharides are permeable to bacterial acids, and from our observations, in spite of the existence of dead layers adjacent to enamel surface, the acidic action did not stop from 4-day specimens, leading to greater accumulations of acid near the surface.

The results of this study suggest that the typical features of carious crystals are observed in the 4-day specimens. The pH of *S. mutans* biofilm and the number and distribution of bacteria on enamel surface have a close relation with enamel crystal demineralization. However, it was suggested that these factors alone are not enough for dental caries to occur. The main factor that integrated all of them was the length of time that the enamel was exposed to biofilm. Enamel crystal demineralization was gradual and progressive over the incubation days, and its interaction with the *S. mutans* biofilm was also a time-related process.

The two most commonly found oral species of mutans streptococci in man are *Streptococcus mutans* and *Streptococcus sobrinus*. In spite of the fact that *S. sobrinus* has been shown to be more acidogenic than other species of mutans streptococci[33], *S. mutans* single-strain biofilm was chosen in this study. The reasons for this were that *S. mutans* has been generally considered to be the prime etiological bacteria of human dental caries[27], and has been found more often and in higher numbers than *S. sobrinus* in the oral cavity[24].

We suppose that the initial evidence of early enamel caries is the demineralization of crystals from enamel surface layer. This demineralization creates a surface layer defective and porous, permitting that the acids produced by bacteria may diffuse more freely along prisms and intercrystal spaces, affecting the enamel subsurface layer. The use of this model of using undecalcified mature enamel sections in conjunction with TEM observation could provide detailed information of the morphological changes and ultrastructural evidence of caries initiation. The use of this new *in vitro* model system could be suitable for verifying how some caries-preventive substances, such as fluoride, xylitol and polyphenol, can inhibit demineralization at the level of enamel crystals and affect the biofilm behavior in the early stages of dental caries. Further studies using *S. mutans* and *S. sobrinus* biofilm and multi-strains biofilm are to be carried out to observe the role of other bacterial strains in enamel crystals demineralization that leads to dental caries.

Acknowledgments

This research was supported in part by a grant-in-aid for scientific research C2 No. 11672039 (1999/2000) from the Japanese Ministry of Education, Culture, Sport, Science and Technology.

References

1. Balakrishnan M, Simmonds RS, Tagg JR. Dental caries is a preventable infectious disease. Aust Dent J 2000; 45 : 235-45.
2. Shu M, Wong L, Miller JH, et al. 2000. Development of multi-species consortia biofilms of oral bacteria as an enamel and root caries model system. Arch Oral Biol 2000 ; 45 : 27-40.
3. Tanzer JM. 1989. On changing the cariogenic chemistry of coronal plaque. J Dent Res 1989 ; 68 : 1576-87.
4. van Houte J. Role of micro-organisms in caries etiology. J Dent Res 1994 ; 73 : 672-81.
5. Fitzgerald RJ, Keyes PH. Demonstration of the etiologic role of streptococci in experimental caries in the hamster. J Am Dent Assoc 1960 ; 61 : 9-19.
6. Gibbons RJ. Formation and significance of bacterial polysaccharides in caries etiology. Caries Res 1968 ; 2 : 164-71.
7. Gibbons RJ, Banghart S. Synthesis of extracellular dextran by cariogenic bacteria and its presence in human dental plaque. Arch Oral Biol 1967 ; 12 : 11-24.
8. Selvig KA. The crystal structure of hydroxyapatite in dental enamel as seem with the electron microscope. J Ultrastructure Res 1972 ; 41 : 369-75.
9. Tohda H, Takuma S, Tanaka N. Intracrystalline structure of enamel crystals affected by caries. J Dent Res 1987 ; 66 : 1647-53.
10. Ichijo T, Yamashita Y, Terashima T. Observations on the structural features and characteristics of biological apatite crystals (2) Observation on the ultrastructure of human enamel crystals. J Med Dent Sci 1992 ; 39 : 71-80.
11. Zahradnik RT, Moreno EC, Burke EJ. Effect of salivary pellicle on enamel subsurface demineralization *in vitro*. J Dent Res 1976 ; 55 : 664-70.
12. Zahradnik RT, Propas D, Moreno EC. *In vitro* enamel demineralization by *Streptococcus mutans* in the presence of salivary pellicles. J Dent Res 1977 ; 56 : 1107-10.
13. Meurman JH, Tuompo H, Lounatmaa K. Ultrastructural visualization of the adherence of *Streptococcus mutans* and *Streptococcus salivarius* to hydroxyapatite. Scand J Dent Res 1983 ; 91 : 447-52.
14. Poole DFG, Brooks AW. The arrangement of crystallites in enamel prisms. Arch Oral Biol 1961 ; 5 : 14-26.
15. Frazier PD. Adult human enamel: an electron microscopic study of crystallite size and morphology. Ultrastructure Res

1968 ; 22 : 1-11.
16. Daculsi G, Kerebel B. High-resolution electron microscope study of human enamel crystallites: size, shape, and growth. J Ultrastruct Res 1978 ; 65 : 163-72.
17. Ichijo T. The ultrastructure of enamel and images of carious enamel. In: Suga S, Ishii T, editors, Caries Susceptibility-structure and Composition of the Enamel Surface, Tokyo : Kokuh Hoken Kyokai, 1976 : 94-116.
18. Ichijo T. On the basic structural features and characteristics of human enamel crystals. Jpn J Oral Biol 1983 ; 25 : 615-34 (in Japanese, English abstract).
19. Ichijo T. Observations on structural features and characteristics of human tooth and bone crystals – the field of view magnified 10,000,000 times. Tokyo : Ishiyaku Publishers, 1995 : 94-116.
20. Scott DB, Simmelink JW, Nygaard V. Structural aspects of dental caries. J Dent Res 1974 ; 53 : 165-78.
21. Takuma S. Demineralization and remineralization of tooth substance – an ultrastructural basis for caries prevention. J Dent Res 1980 ; 59 : 2146-56.
22. Ichijo T, Yamashita Y, Terashima T. Observations on structural features and characteristics of biological apatite crystals (9) Observation on dissolution of carious enamel crystals. J Med Dent Sci 1994 ; 41 : 1-13.
23. Johnson NW. Some aspects of the ultrastructure of early human enamel caries seen with the electron microscope. Arch Oral Biol 1967 ; 12 : 1505-21.
24. Lindquist B, Emilson C. Dental location of *Streptococcus mutans* and *Streptococcus sobrinus* in humans harboring both species. Caries Res 1991 ; 25 : 146-52.
25. Robinson C, Weatherell JA, Kirkham J. The chemistry of dental caries. In: Robinson C, Kirkham J, Shore R, editors, Dental Enamel – Formation to Destruction, Boca Raton : CRC Press, 1995 : 223-43.
26. Geddes DAM. Acids produced by human dental plaque metabolism in situ. Caries Res 1975 ; 9 : 98-109.
27. van Houte J, Sansone K, Joshipura K, et al. *In vitro* acidogenic potential and mutans streptococci of human smooth-surface plaque associated with initial caries lesions and sound enamel. J Dent Res 1991 ; 70 : 1497-502.
28. van Ruyven FOJ, Lingström P, van Houte J, et al. Relationship among mutans streptococci, “low-pH” bacteria, and iodophilic polysaccharide-producing bacteria in dental plaque and early enamel caries in humans. J Dent Res 2000 ; 79 : 778-84.
29. Netuschil L, Reich E, Unteregger G, et al. A pilot study of confocal laser scanning microscopy for the assessment of undisturbed dental plaque vitality and topography. Arch Oral Biol 1998 ; 43 : 277-85.
30. Auschill TM, Artweiler NB, Netuschil L, et al. Spatial distribution of vital and dead microorganisms in dental biofilms. Arch Oral Biol 2001 ; 46 : 471-76.
31. Margolis HC, Murphy BJ, Moreno EC. Development of carious-like lesions in partially saturated lactate buffers. Caries Res 1985 ; 19 : 36-45.
32. Dibdin GH, Wilson CM, Shellis RP. Effect of packing density and polysaccharide to protein ratio of plaque samples cultured in vitro upon their permeability. Caries Res 1983 ; 17 : 52-8.
33. De Soet JJ, Toors FA, De Graaff J. Acidogenesis by oral streptococci at different pH values. Caries Res 1989 ; 23 : 14-7.